Inhibition recruitment in prefrontal cortex during sleep spindles and gating of hippocampal inputs

Adrien Peyrache[a,1,2], Francesco P. Battaglia[b], and Alain Destexhe[a]

[a]Neuroscience, Information and Complexity Unit, UPR 3293, Centre National de la Recherche Scientifique, 91198 Gif-sur-Yvette, France; and [b]Center for Neuroscience, Swammerdam Institute for Life Sciences, Faculty of Science, University of Amsterdam, 1090 GE, Amsterdam, The Netherlands

Edited by Terrence J. Sejnowski, The Salk Institute for Biological Studies, La Jolla, CA, and approved August 24, 2011 (received for review March 7, 2011)

During light slow-wave sleep, the thalamo-cortical network oscillates in waxing-and-waning patterns at about 7 to 14 Hz and lasting for 500 ms to 3 s, called spindles, with the thalamus rhythmically sending strong excitatory volleys to the cortex. Concurrently, the hippocampal activity is characterized by transient and strong excitatory events, Sharp-Waves-Ripples (SPWRs), directly affecting neocortical activity—in particular the medial prefrontal cortex (mPFC)—which receives monosynaptic fibers from the ventral hippocampus and subiculum. Both spindles and SPWRs have been shown to be strongly involved in memory consolidation. However, the dynamics of the cortical network during natural sleep spindles and how prefrontal circuits simultaneously process hippocampal and thalamo-cortical activity remain largely undetermined. Using multisite neuronal recordings in rat mPFC, we show that during sleep spindles, oscillatory responses of cortical cells are different for different cell types and cortical layers. Superficial neurons are more phase-locked and tonically recruited during spindle episodes. Moreover, in a given layer, interneurons were always more modulated than pyramidal cells, both in firing rate and phase, suggesting that the dynamics are dominated by inhibition. In the deep layers, where most of the hippocampal fibers make contacts, pyramidal cells respond phasically to SPWRs, but not during spindles. Similar observations were obtained when analyzing γ-oscillation modulation in the mPFC. These results demonstrate that during sleep spindles, the cortex is functionnaly "deafferented" from its hippocampal inputs, based on processes of cortical origin, and presumably mediated by the strong recruitment of inhibitory interneurons. The interplay between hippocampal and thalamic inputs may underlie a global mechanism involved in the consolidation of recently formed memory traces.

cortical deafferentation | fast spiking neurons | regular spiking neurons | memory reprocessing | Up and Down states

Slow-wave sleep (SWS) is thought to be determinant for memory consolidation (1) but the ongoing brain dynamics in this stage and the interaction between the cortex and subcortical structures are still largely unknown. During SWS, the neocortex is dominated by fluctuations between active and silent phases at approximatively 0.1 to 1 Hz, the so-called "slow oscillations" (2). These slow waves modulate nested faster oscillatory events in the thalamus and the hippocampus, which in turn produce strong excitatory volleys directly targeting the neocortical network. In light stages of SWS, the thalamo-cortical network exhibits episodes of waxing-and-waning spindle oscillations, at about 7 to 14 Hz and lasting for 500 ms to 3 s (3), during which neocortical networks receive rhythmic and strong excitatory volleys from the thalamo-cortical cells (3, 4). From a functional point of view, the density of spindle events have been shown to correlate with memory enhancement (5, 6).

In parallel to spindles, the hippocampus produces brief bursts of activity associated with fast oscillations at about 200 Hz in the CA1 subfield (7), the so-called "Sharp-Waves Ripple" complexes (SPWRs). Sleep SPWRs replay activity patterns related to past experience (8) and are involved in the long-term storage of memories (9). The thalamus projects directly to every part of the neocortex, in a distributed, topographically organized fashion different for each thalamic nucleus, but in rodents the hippocampus efferents preferentially target the medial prefrontal cortex (mPFC) (10). In fact, the hippocampus and mPFC interact both during wakefulness (11, 12) and during SWS, when mPFC neuronal activity replay activity patterns formed during previous learning experience (13, 14).

GABAergic interneurons represent approximatively 20% of the neurons in the neocortex and are very diverse in nature (15). Both pyramidal and local GABAergic neurons are directly targeted by thalamic (16) and, in the mPFC, hippocampal (17, 18) glutamatergic afferents, such that thalamo-cortical as well as hippocampal inputs provoke an excitatory postsynaptic potential (EPSP)/inhibatory postsynaptic potential (IPSP) sequence in neocortical pyramidal neurons (17, 19). Indeed, during spindles under barbiturate anesthesia, intracellular recordings in the neocortical pyramidal cells reveal subthreshold EPSP/IPSP sequences with powerful inhibition (19). Similarly, electrical stimulation in the hippocampus provoke a reliable and large activation of the prefrontal interneurons (18). Consequently, interneurons are thought to play a key role in shaping pyramidal response in the mPFC, possibly controlled by different neuromodulators, such as dopamine (12, 20). Moreover, the interaction in local networks between GABAergic fast-spiking (FS) and regular-spiking (RS) cells, underlying information processing, is thought to be instrumental in the transient formation of cell assemblies (12, 21) associated with γ-oscillations (22).

Although targeting both pyramidal cells and interneurons, thalamic and hippocampal inputs to the mPFC are differently distributed: the ventral CA1 area of the hippocampus targets primarily the deep layers (10) and the mediodorsal nucleus of the thalamus, which is the primary thalamic afferent of the mPFC, mostly projects to Layer III (23). Here, we investigate how the mPFC process these different inputs during SWS by analyzing the response and integration of the different cell types and layers, as well as the γ-oscillation profiles during those perturbations.

Results

Different Recruitment and Phase Modulation Across Layers During Spindling. During spindling episodes, mPFC local field potentials (LFP) exhibited large amplitude oscillations identifiable as low-voltage sleep spindles, based on several physiological criteria (Fig. 1*A* and *SI Materials and Methods*). When the LFPs were recorded simultaneously in superficial and deep layer FS (in three rats), a phase inversion was observed between layers (Fig. S1). Herein, if not stated otherwise, spindle phases will refer to deep prefrontal LFPs. FS and RS cells were discriminated on the basis of the shape of their action potential (*SI Materials and Methods* and Fig. S2). Their responses were different depending

Author contributions: A.P. and A.D. designed research; A.P. and F.P.B. performed research; A.P., F.P.B., and A.D. analyzed data; and A.P., F.P.B., and A.D. wrote the paper.

The authors declare no conflict of interest.

This article is a PNAS Direct Submission.

[1]To whom correspondence should be addressed. E-mail: adrien.peyrache@gmail.com.

[2]Present address: Center for Molecular and Behavioral Neuroscience, Rutgers, State University of New Jersey, Newark, NJ 07102.

This article contains supporting information online at www.pnas.org/lookup/suppl/doi:10.1073/pnas.1103612108/-/DCSupplemental.

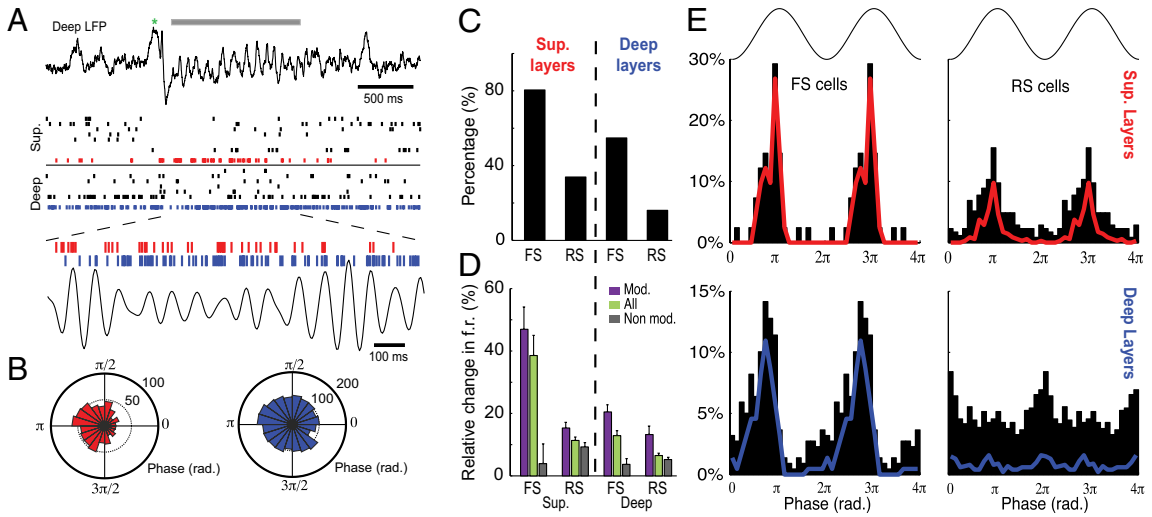

Fig. 1. Interneuron and superficial pyramidal cell recruitment during spindles. (*A* and *B*) Example of neuronal recruitment by spindles by layers. (*A*) Deep LFP trace (*Upper*) shows a transient bout of waxing-and-waning oscillations at about 15 Hz, the spindle oscillations, denoted by the horizontal gray bar; below: raster of discriminated units spiking activity in the superficial layers (II/III) and deep layers (V/VI). Firing from two FS cells, one in each layer, is depicted here in color and RS cell spikes are displayed in black. Note the δ-wave preceding the spindles (green asterisk). (*Lower*) An enlarged picture of the spindle oscillation: filtered deep LFP trace (10–15 Hz) is shown together with the spiking activity of the same FS cells as above. (*B*) Phase histogram of the example FS cells from *A* relative to spindle oscillations (same color code). (*C*) Percentage of significantly phase modulated cells. (*D*) Average relative change in firing rate during spindle oscillations compared with nonspindle SWS for significantly phase-locked cells (Mod., purple) or not (Non mod., gray) and for all of the cells (All, green) changed to green. Error bars display SEM. (*E*) Distributions of preferred firing phase of cells. Black bars indicate preferred phase for all cells; distributions for significantly phase-modulated cells only are shown in color lines.

on the layer from which they were recorded. In the example shown in Fig. 1*A*, two FS cells were recorded from the two layers, respectively: although the deep-layer cell showed a slight increase in firing rate during the spindling episode, the superficial-layer cell is transiently and strongly activated. Moreover, histograms of action potential phase relative to band-pass filtered LFP in the spindle band (10–15 Hz) revealed a strong phase modulation of the superficial FS cell ($P < 10^{-10}$, $\kappa = 6.2$, Rayleigh test) and a weaker but still significant modulation for the deep FS cell ($P < 10^{-10}$, $\kappa = 2.6$, Rayleigh test).

Although the deep-layer LFP was taken as reference, a larger fraction of superficial cells were phase-modulated than deep-layer cells, both for FS (80% vs. 55%, $P < 10^{-10}$, binomial test) and RS (34% vs. 16%, $P < 10^{-10}$) neurons (Fig. 1*C*). However, a cell can increase its firing rate during spindles without any phase-locking. Fig. 1*D* shows that although all cell types showed an increase of their relative firing rate, that is the difference between rates within and outside spindles divided by rates outside spindles (the latter being restricted to SWS epochs, see *SI Materials and Methods*), this was consistently higher for those cell types that were phase-modulated ($P < 0.01$ for all cell types, two-sample *t* test). Moreover, the same difference across layers and cell types were observed as with phase-modulation: in a given layer, FS cells tend to consistently be more recruited ($P < 10^{-10}$, two-way ANOVA), and superficial layers exhibited a stronger activation ($P < 10^{-10}$). However, the interaction between cell types and layers was also significant ($P < 10^{-5}$), showing that the difference between cell types was more marked in the superficial layers than in the deep layers ($P < 10^{-10}$ and $P < 0.001$, post hoc *t* test, respectively). Moreover, both FS and RS increased their firing rate more in the superficial than in the deep layers ($P < 10^{-7}$ and $P < 0.001$, post hoc *t* test, respectively).

Example neurons from Fig. 1*B* tend to fire at the peak of the LFP. This feature was indeed present at the population level: FS cells in both layers fire preferentially at the peak of the oscillation (Fig. 1*E*). Superficial RS cells showed the same preferred phase. Conversely, the small percentage of significantly modulated deep-layer RS cells (16%) did not show any particular preferred phase. Nevertheless, as a population, deep RS cells tended to fire at the peak of the spindle oscillations ($P < 0.001$, Rayleigh test). Similar results, but in antiphase, were obtained when superficial LFPs were taken as reference (Fig. S3).

Grouping of Thalamic and Hippocampal Activity Bursts by the Slow Oscillations. During SWS, hippocampal activity is concentrated in SPWR events, the occurrence of which is modulated by neocortical inputs (24). Similarly, during light SWS, neocortical DOWN to UP state transitions favor the recruitment of thalamic activity into spindles (3). Cortical δ-waves, large and isolated deflection of the LFP, are the hallmark of global or local DOWN states and are referred to as K-complex when followed by spindles (as indicated with a green asterisk in Figs. 1*A* and 2*A*). As suggested by the example shown in Fig. 2*A*, δ-waves were preceded by an increased probability of SPWR occurrence (or conversely, some SPWRs tended to take place at the end of UP states), and the stronger the deflection, the higher the propensity of SPWR occurrence (Fig. 2*B*, *Upper*, black arrow). However, δ-waves were also followed by an increased occurrence rate of SPWRs, albeit smaller than the rate right before DOWN states (white arrow). Similarly, there was a tendency for δ-waves to be followed by spindles (Fig. 2*B*, *Lower*), also in an amplitude-dependent manner. This temporal ordering was reflected in the asymmetric SPWR-triggered spindle density over timescales spanning at least four order-of-magnitude, from subsecond to minutes (Fig. 2*C*) (cf. 25, 26). Hippocampal burst amplitude can modulate differently PFC response, especially in the spindle band (27). Indeed, the strongest SPWRs, as measured by the amplitude of ripple oscillations (*SI Materials and Methods*), were followed by higher spindle peak occurrence rate than the smallest ones (Fig. S4*A*). However, the relationship between SPWRs and δ-waves did not show such dependence (Fig S4*B*).

Neuronal Sensitivity to Hippocampal Sharp-Waves Depends on Cortical State. SPWR-associated activity directly impinges upon prefrontal neuronal activity (14, 27). However, it is not known whether cells in different cortical layers respond differentially to SPWRs, or whether this response is state-dependent. Qualitative examination of cross-correlogram of neuronal activity for the two

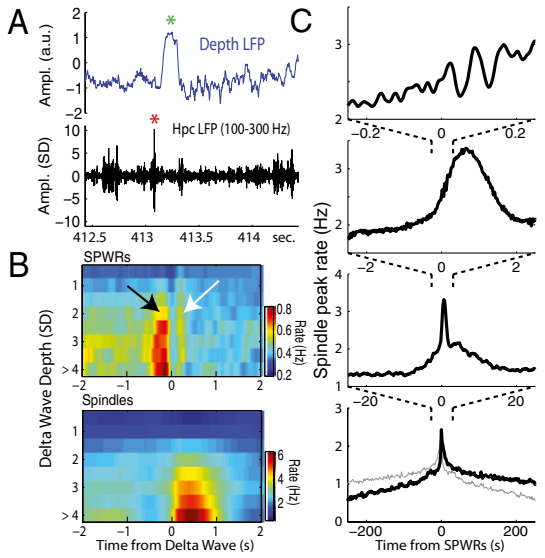

Fig. 2. Interrelationship between SPWRs, spindles, and the neocortical slow oscillation at various timescales. (*A*) Example of simultaneous unfiltered mPFC LFP (*Upper* trace, green asterix indicates a δ-wave) and hippocampal LFP in the pyramidal layer filtered in the ripple band (*Lower* trace, red asterix indicates a detected SPWR; signal is *z*-scored). (*B*) Cross-correlograms of δ-waves (reference) and SPWRs occurrence time in function of depth of the δ-wave (expressed in *z*-score of the filtered LFP in the 0.1–4 Hz band) (*SI Materials and Methods*). All δ-waves above 4 SD are grouped in the last row. Colors indicate occurrence rate. (*B*) Same as *A* but for spindle peaks. (*C*) Cross-correlograms between SPWRs (reference) and spindle peaks at various timescales, from fine (*Top*) to long timescales (*Bottom*). The thin gray line in the bottom panel is the time-reversed correlogram displayed to emphasize the difference between negative (*Left*) and positive (*Right*) time-lag differences. Only long SWS episodes (>12 min) were used for the last cross-correlation.

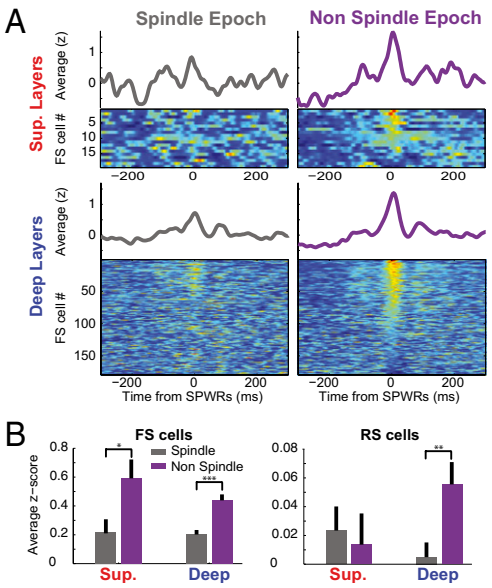

Fig. 3. Prefrontal cells enhanced responsiveness to hippocampal SPWRs during rather than outside spindle episodes. (*A*) Average (*Upper*) and individual (*Lower*) *z*-scored cross-correlograms of superficial FS cells relative to SPWRs occurrence time during spindle oscillation episodes (*Left*) and nonspindle state (*Right*). Cells are ordered relative to the strength of activation during non spindle states. (*B*) Summary statistics of FS cell (*Left*) and RS cell (*Right*) modulation by SPWRs. Cross-correlograms were *z*-scored on a ± 400-ms window around SPWRs and averaged over a ± 40-ms window (**P* = 0.026, ***P* = 0.0018, ****P* < 10^{-9}; paired *t* test).

cell types and layers (Fig. S5), within or outside spindle episodes, revealed strikingly different responses. First, SPWR that occurred during spindle episodes are associated with an ongoing state of elevated neuronal firing (suggested by the symmetric modulation in the cross-correlogram). This finding is most remarkable for superficial FS and RS cells, and is compatible with the large, UP state-related dipole measured in superficial layers (28). Indeed, in deep layer this effect is weaker, and virtually absent for RS cells. Second, during nonspindling-associated SPWR events, cortical activity displayed a transient increase, followed by a longer-lasting (1–2 s) plateau of elevated activity compatible with the relationship between SPWRs and UP state onset occurring after δ-waves (Fig. 2*A*) (26, 29). However, deep-layer RS cells show only a transient firing increase, and no sustained activation (Fig. S5).

Finer examination of the relationship of prefrontal spiking activity with SPWR depending on the spindling state revealed first that FS cells were the most activated. Individual and population average *z*-scored cross-correlograms in a ± 400-ms window (Fig. 3*A*) showed that their sensitivity to SPWR relatively to their ongoing firing was enhanced during non spindling states by a factor of 2 to 3 (Fig. 3*B*, *Left*) (superficial FS: $P < 0.05$; deep FS: $P < 10^{-10}$, paired *t* test). Furthermore, only deep-, and not superficial-, layer RS cells showed a significant transient response to SPWRs (Fig. 3*B*, *Right*). However, during spindling episodes, this response vanished.

State-Dependent γ-Response. γ-Rhythms in rodent neocortex span a wide range of frequency, from 30 to 140 Hz (30). The example in Fig. 4 shows that γ-oscillations occur in bursts of various frequencies that tended to fire at the peaks of the deep LFP spindle oscillation. We analyzed how instantaneous broadband γ-power (30–140 Hz) changed in relation with spindle and SPWRs. First, γ-power was strongly modulated in phase by spindles, as measured by the averaged *z*-scored cross-correlogram in ± 500-ms windows (Fig. 5*A*). The power spectra of instantaneous wide-

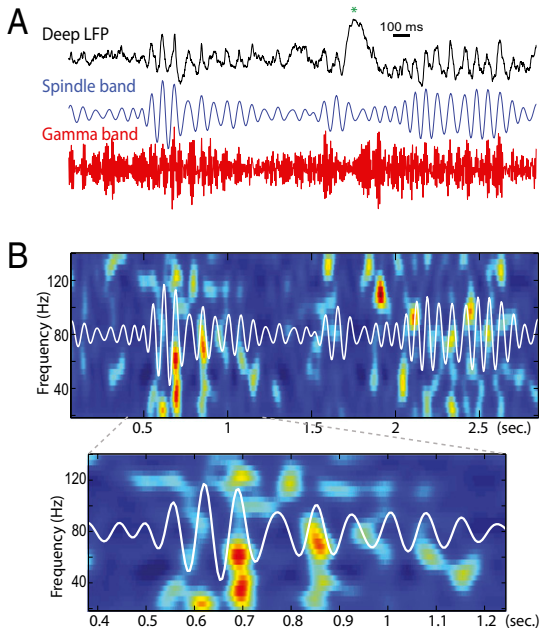

Fig. 4. Example of phase-relationship between spindle oscillations and γ-burst in the mPFC. (*A*) Raw LFP trace (*Top*, black) filtered in the spindle band (*Middle*, blue), and 30- to 140-Hz γ-band (*Bottom*, red). The green asterisk indicates a δ-wave. (*B*) Time-frequency analysis in the γ-band reveals the occurrence of γ-bursts at different frequencies that tend to appear at the peak of the deep-layer spindle oscillations, as shown in the enlarged panel.

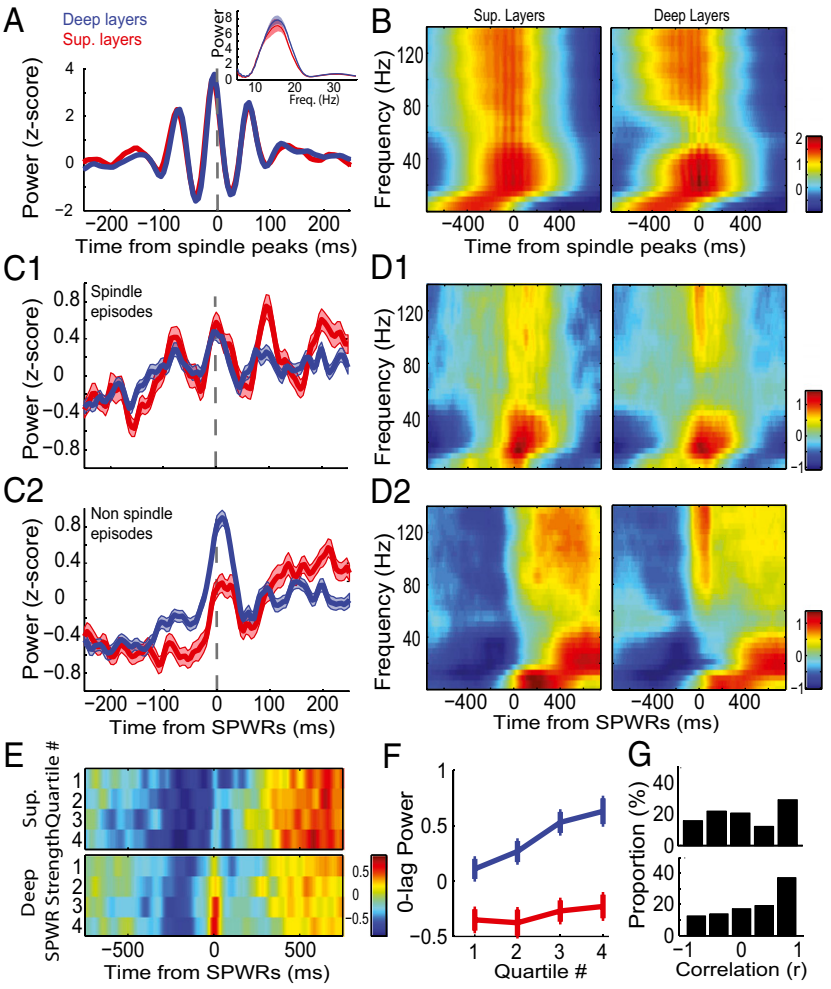

Fig. 5. γ-Recruitment in the mPFC during spindles and SPWRs. (*A* and *B*) γ-Modulation by spindle oscillations: broadband (30–140 Hz) γ-power (average of *z*-scored cross-correlograms, *A*) and LFP spectogram triggered on spindle peaks (*z*-scored for each frequency band in a ± 750-ms window), in deep (blue) and superficial (red) layers. Inset in *A* shows the power spectra (in arbitrary units) of the averaged γ-power shown in *A*. Shaded areas indicate 95% confidence intervals (Jackknife bootstrap). (*C1* and *D1*) Same as *A* and *B* but triggered on SPWRs during spindling episodes. (*C2* and *D2*) Same as *C1* and *D1* but during nonspindling epochs. (*E*) Wide-band γ-response to SPWRs outside spindle episodes in function of SPWR strength quartile (*SI Materials and Methods*) in the superficial (*Upper*) and deep (*Lower*) layers. (*F*) Zero-lag γ-power (averaged in a ± 20-ms window) in function of SPWR strength quartiles. (*G*) Distribution of correlation coefficients between γ-amplitude change at 0-lag (computed as in *F*) with SPWR quartiles across all LFP signals measured in the superficial (*Upper*) and deep layers (*Lower*). Shaded areas in *A*, *C*, and *E*, and error bars in *F* display SEM.

band γ-power (Fig. 5*A*, *Inset*), quantifying the depth of modulation by spindles, were not different in the deep and superficial layers ($P > 0.05$, Jackknife). Moreover, the power spectra in the γ-band revealed an increase in all γ-frequency bands, with a stronger effect in the 30- to 50-Hz band compared with faster γ-oscillations (>70 Hz) (Fig. 5*B*). We then analyzed how SPWRs related to γ-oscillations. During spindling episodes, γ-oscillations were modulated by SPWRs, as well as by the spindle cycle. The effect was not different in the two layers and was at about 0.5 SD over the baseline (Fig. 5*C1*). However, the rythmic modulation could be a by-product of phase-locking of SPWRs to spindles (Fig. 2*C*) (see also refs. 25 and 26). Conversely, during nonspindling episodes, SPWRs were preceded by a state of weak γ-activity (Fig. S6)—most probably the end of the previous UP state—and provoked a rebound, especially in the deep layers (Fig. 5*C2*). Interestingly, the γ activation was not the same in all frequency bands (Fig. 5*D2*): slow γ (30–50 Hz) band power increased sustainably with a 400-ms delay after SPWR occurrence in both layers, and fast γ (>70 Hz) was evoked transiently in the deep layers, possibly caused by (or at least correlated with) spiking itself (Fig. S7). Finally, in the deep layers, wide-band γ-power at the time of SPWR occurrence increased with SPWR strength (Fig. 5 *E* and *F*). When taken individually (Fig. 5*G*), 61% of deep-layer LFPs showed correlated wide-band γ-response with SPWR strength ($P < 0.001$, $n = 151$ LFP channels, binomial test), whereas only 49% of superficial LFPs did so ($n = 82$, not significant from chance level). This increase of wide-band γ-power was specifically the consequence of increase high γ-power (Fig S4*C*). If SPWR strength was significantly stronger outside rather than within spindle episodes ($P < 0.01$, paired *t* test), the relative increase of ripple-frequency band power was too low (1.3% in average) to explain the observed differences in PFC activity between the two conditions.

Discussion

Taking advantage that the PFC receives afferents from both hippocampus and thalamus, we investigated the dynamic recruitment of cortical cells into thalamo-cortical and hippocampo-cortical assemblies during SWS. Discrimination between FS and RS cells and fine histological reconstruction of electrode tracks allowed the examination of the response and interaction of these different cell types and cortical layers to thalamic and hippocampal inputs.

Rhythmic Activation of Neocortical FS Cells During Spindle Oscillations. We investigated the interaction between thalamo-cortical spindles and hippocampal SPWRs onto the mPFC. Although it is possible that the analyzed oscillations could be better classified as high-voltage spindles, this is unlikely because several physiological parameters pointed in favor of natural sleep spindles (*SI Materials and Methods*). These low-voltage spindle oscillations are the hallmark of thalamo-cortical assembly recruitment during the light stages of SWS (3, 31), with thalamo-cortical cells bursting and depolarizing neocortical dendrites. FS cells were strongly modulated by spindle oscillations, both in their phases and in firing rates. Whereas superficial RS cells were also recruited, deep-layer RS cells were phase-modulated poorly, if at all (Fig. 1). This population shows a slight tendency for firing

preferentially in antiphase with all other cells, in particular deep FS, and would thus fire when the local inhibition is the lowest. These results are in agreement with several other previous findings. First, the higher modulation of superficial cells by spindles is consistent with the denser projection from the main projecting thalamic input, namely the medio-dorsal nucleus, to the superficial layers of the mPFC (23). Second, spindle synchronization requires the intact thalamo-cortical system (32), with a prominent synchronizing role of cortico-cortical projections in the superficial layers (33). Third, in intracellular recordings during spindle oscillations, the weak modulation in control conditions was changed to powerful bursts by using Cl-filled pipettes, revealing strong inhibition (19).

A recent study reported that a class of superficial FS cells, namely the dendritic targeting cells, fire in antiphase with local pyramidal neurons (34). No such cells were found in our dataset but this might be explained by the lack of very superficial-layer recordings where these cells were found.

Modulation of γ-Burst Occurrence by Spindle Oscillations. In many ways, UP states are similar to waking desynchronized states, in particular because neocortical neurons display similar patterns of correlation and conductances (35), and γ-oscillations in the LFPs (36). γ-Oscillations are associated to the activation of neocortical cell assemblies (22, 37) and are probably caused by strong interactions between FS and RS cells or between FS cells only (38, 39). Here we show that mPFC γ-activity (30–140 Hz) was remarkably modulated by spindle oscillations (Fig. 5*A*).

Interestingly, the hippocampal θ-rhythm (5–10 Hz) of active behavior modulates γ-bursts in a similar way: local γ-bursts in CA1 (40, 41) as well as neocortical γ-bursts (30, 42) are phase-locked to the θ-oscillation. The modulation of local fast events by remote slower oscillations is thus a common mode of inter-structure communication mechanisms, both between the thalamus and neocortex, and between the hippocampus and neocortex (43, 44).

Interaction Between Thalamic and Hippocampal Inputs at Multiple Timescales. During SWS, the hippocampal influence on mFPC is mostly mediated by SPWRs, whose occurrence is in turn modulated by the slow oscillation and its nested rhythms: δ- and spindle oscillations (24–26, 29). We provided further data on how these different comodulated events may interact.

SPWR influence on mPFC activity depended on the neocortical state and in particular its oscillatory drive from the thalamus: mPFC sensitivity to hippocampal SPWRs was greater when the mPFC was not involved in thalamo-cortical coupling (Figs. 3 and 5). In particular, deep-layer RS cells relayed hippocampal inputs preferentially during nonspindle states, when they are released from thalamic drive. In this state, SPWRs were concomitant with short (<100 ms) fast γ-bursts (>70 Hz) in the deep layers and the amplitude of the response was correlated to SPWR strength (Fig. 5 *E*–*G* and Fig. S4), pointing at activation of the deep layers: fast-γ is strongly related to spiking activity (Fig. S7), possibly because of the low-frequency component of action potentials leaking in the LFP (45). In general, outside spindling episodes SPWRs tended to appear toward the end of UP states, as shown by (*i*) the low spiking (Fig S5 and ref. 29), (*ii*) low γ-activity (Fig. 5 and Fig. S6) preceding these SPWRs, and (*iii*) the negative time-lag shift of the maximum peak in the the correlation between δ-waves and SPWRs (Fig. 2*B*, black arrow). At the end of UP states, global activity decreases leading to enhanced cell input resistance (46, 47). This process may favor enhanced responsiveness of mPFC cells to hippocampal inputs. However, the SPWRs–δ-wave correlation shows another, but smaller, peak for positive time-lag (Fig. 2*B*, white arrow). This finding indicates that both UP-DOWN and DOWN-UP transitions could be associated to SPWR occurrence. Whether the hippocampus passively reacts to its inputs or plays an active role in neocortical-state transitions, through mechanisms similar to what shown in vitro (47), remains to be determined (24–26, 29). Note that δ-wave strength was only correlated with the occurrence rate of SPWRs preceding them, suggesting that hippocampal input may be important for complete termination of activity during DOWN states. The second peak, at the putative DOWN-UP transition, was of comparable strength for all δ-waves. Although the present dataset focused on an output structure of the hippocampus, the mPFC, it would be interesting to study how the δ-wave strength in the up-stream areas (i.e., the entorhinal cortex) would affect SPWR occurrence.

SPWRs and spindles are highly comodulated events (25, 26). The PFC's response is positively correlated with the strength of the SPWR, as measured by hippocampal population activity (27). Strong SPWR events were clearly associated to increased occurrence rate of spindle peaks (Fig S4*A*). Such a relationship was absent between SPWR and δ-waves (Fig S4*B*). One possibility would be that SPWRs can themselves recruit thalamo-cortical cells into a spindling episodes in a strength-dependent fashion, in a way similar to the neocortical synaptic barrage associated to UP state onset (3).

Furthermore, we show that the timescales of the interaction between the SPWRs and spindle events spanned several orders of magnitude (Fig. 2*C*). SPWRs were phase-locked to spindles (26), but at larger timescales SPWRs preceded spindle occurrence (25), possibly because of common modulation by the slow oscillation (3, 24, 26, 29), in particular its DOWN phase (Fig. 2*B*), and possibly to lower frequency components in the SWS dynamics.

Cortical Deafferentiation During Spindles. Thalamo-cortical cells have roughly two modes of activity, phasic or bursting, and the latter is thought to be responsible for the disruption of relay property of thalamo-cortical cells (3). However, the present study proposes an alternative view. The monosynaptic hippocampo-prefrontal projection offers a unique chance to study the response of a cortical area to an endogenous stimulation independent of the thalamic relay. The present results demonstrate that the cortex is generally unresponsive during spindles, suggesting that thalamic inputs in burst mode recruit massive intracortical inhibition, which itself produces a local deafferentation of the cortical area concerned, regardless of the input source.

Implications for Memory Formation. The communication between the mPFC and the hippocampus are likely to be crucial for memory formation and consolidation (48). Based on our data, some hypotheses may be drawn about the functional implications of neural dynamics in these areas. Excitatory input from thalamo-cortical cells is thought to massively depolarize neocortical cell dendrites during spindles (19). This finding was suggested to play a role in plasticity mechanisms by enabling calcium entry in dendrites and mobilizing molecular mechanisms for stable changes in synaptic weights (19, 31). On the other hand, to consolidate a given memory trace networks must avoid interference from their spontaneous activity dynamics. Perisomatic inhibition (of which we show the possible effects), would then be the key factor in permitting dendritic depolarization yet in keeping pyramidal cell activity under tight control. However, this theory does not explain which memory trace would be consolidated through this process. During wakefulness, mPFC neuronal activity self-organizes in cell assemblies that are reactivated during sleep (13), preferentially at times of hippocampal SPWRs (14). SPWRs tend to precede spindles over multiple time scales (Fig. 2*C*), and cell-assembly replay likely occurs at the same times (14). Thus, a likely sequence of events would see replay first (coincident with SPWRs), and then a state favoring consolidation of the recently modified synapses, during spindles.

This theory would explain why during slow oscillations, which temporally organize the chain of events described above, replay is indeed enhanced (6, 14). Thus, although at a subsecond timescale spindles do not corresponds to peaks in replay (14) or hippocampal/PFC communication (shown here), a positive correlation is found at a longer (minutes) timescale between spin-

dling activity and replay (6). Similarly, spindling EEG power is increased with learning (5), possibly as a result of a general increase in slow oscillation activity (49).

This hypothetical gating effect of thalamo-cortical inputs between hippocampal-triggered vs. intrisically cortical consolidation processes would be mediated by the prefrontal cortex circuitry, as we show here, with distinctive roles for FS and RS cells in different layers. The functional importance of this structure will have to be investigated in future work.

Materials and Methods

Four Long-Evans (pigmented) male rats (R. Janvier) weighing 250 to 300 g at arrival, were handled daily. All experiments were carried out in accordance with institutional (Centre National de la Recherche Scientifique Comite Operationnel pour l'Ethique dans les Sciences de la Vie) and international (National Institutes of Health) standards and legal regulations (Certificate no. 7186, French Ministere de l'Agriculture et de la Peche) regarding the use and care of animals. After habituation to the experimental environment, rats were anesthetized with intramuscular xylazine (Rompun, 0.1 mL) and intraperitoneal pentobar-bital (35 mg per kilogram of body weight). A drive containing seven tetrodes (six recording plus one reference) was implanted through the skull above the right mPFC (anterior-posterior, 3.55 mm; medial-lateral, 0.51.5 mm). Each tetrode was contained in a 30-gauge hypodermic tube, with the tubes arranged in two parallel, adjacent rows. Tetrodes were twisted bundles of polymide-coated nichrome wire (13 mm in diameter; Kanthal); the drive allowed independent adjustment of tetrode depth. After dura retraction, two rows of cannulae were implanted parallel to the sagittal sinus so that they targeted the superficial and deep layers of the medial bank of the cortex. A separate microdrive containing three tetrodes was targeted to the ventral hippocampus (anterior-posterior, 5.0 mm; medial-lateral, 5.0 mm). Each tetrode was electrically connected in a single-electrode configuration (all channels shorted together) and used for LFP recordings. A screw implanted on the occipital bone above the cerebellum served as the LFP reference. The hippocampal tetrodes were lowered to the CA1 pyramidal layer; the depth was adjusted with the help of LFP signs (flat sharp waves, strong ripple oscillations). After surgery, rats recovered for at least 2 wk and the tetrodes were lowered to reach the prelimbic area (main drive) and the CA1 pyramidal layer (hippocampal microdrive). Between sessions, tetrodes were gradually lowered to probe different dorso-ventral levels in the prelimbic area.

See *SI Materials and Methods* for further details.

ACKNOWLEDGMENTS. The authors thank S. I. Wiener, M. Khamassi, and K. Benchenane for help with the experiments; S. Doutremer for histology; D. A. Hopkins and N. Quenechdu for the anatomical reconstructions; and A. Grosmark for careful reading of the manuscript. This work was supported by the Centre National de la Recherche Scientifique, the Agence Nationale de la Recherche (HR-Cortex), and the European Community (BrainScales).

1. Walker MP, Stickgold R (2006) Sleep, memory, and plasticity. *Annu Rev Psychol* 57: 139–166.
2. Steriade M, Nuñez A, Amzica F (1993) A novel slow (< 1 Hz) oscillation of neocortical neurons in vivo: Depolarizing and hyperpolarizing components. *J Neurosci* 13:3252–3265.
3. Steriade M (2003) *Neuronal Substrates of Sleep and Epilepsy* (Cambridge Univ Press, Cambridge, United Kingdom).
4. Kandel A, Buzsáki G (1997) Cellular-synaptic generation of sleep spindles, spike-and-wave discharges, and evoked thalamocortical responses in the neocortex of the rat. *J Neurosci* 17:6783–6797.
5. Gais S, Mölle M, Helms K, Born J (2002) Learning-dependent increases in sleep spindle density. *J Neurosci* 22:6830–6834.
6. Johnson LA, Euston DR, Tatsuno M, McNaughton BL (2010) Stored-trace reactivation in rat prefrontal cortex is correlated with down-to-up state fluctuation density. *J Neurosci* 30:2650–2661.
7. Buzsáki G, Horváth Z, Urioste R, Hetke J, Wise K (1992) High-frequency network oscillation in the hippocampus. *Science* 256:1025–1027.
8. Wilson MA, McNaughton BL (1994) Reactivation of hippocampal ensemble memories during sleep. *Science* 265:676–679.
9. Girardeau G, Benchenane K, Wiener SI, Buzsáki G, Zugaro MB (2009) Selective suppression of hippocampal ripples impairs spatial memory. *Nat Neurosci* 12:1222–1223.
10. Jay TM, Witter MP (1991) Distribution of hippocampal CA1 and subicular efferents in the prefrontal cortex of the rat studied by means of anterograde transport of *Phaseolus vulgaris*-leucoagglutinin. *J Comp Neurol* 313:574–586.
11. Siapas AG, Lubenov EV, Wilson MA (2005) Prefrontal phase locking to hippocampal theta oscillations. *Neuron* 46:141–151.
12. Benchenane K, et al. (2010) Coherent theta oscillations and reorganization of spike timing in the hippocampal-prefrontal network upon learning. *Neuron* 66:921–936.
13. Euston DR, Tatsuno M, McNaughton BL (2007) Fast-forward playback of recent memory sequences in prefrontal cortex during sleep. *Science* 318:1147–1150.
14. Peyrache A, Khamassi M, Benchenane K, Wiener SI, Battaglia FP (2009) Replay of rule-learning related neural patterns in the prefrontal cortex during sleep. *Nat Neurosci* 12:919–926.
15. Markram H, et al. (2004) Interneurons of the neocortical inhibitory system. *Nat Rev Neurosci* 5:793–807.
16. Jones EG (1985) *The Thalamus* (Cambridge Univ Press, Cambridge, United Kingdom).
17. Dégenètais E, Thierry AM, Glowinski J, Gioanni Y (2003) Synaptic influence of hippocampus on pyramidal cells of the rat prefrontal cortex: An in vivo intracellular recording study. *Cereb Cortex* 13:782–792.
18. Tierney PL, Dégenètais E, Thierry A-M, Glowinski J, Gioanni Y (2004) Influence of the hippocampus on interneurons of the rat prefrontal cortex. *Eur J Neurosci* 20:514–524.
19. Contreras D, Destexhe A, Steriade M (1997) Intracellular and computational characterization of the intracortical inhibitory control of synchronized thalamic inputs in vivo. *J Neurophysiol* 78:335–350.
20. Tierney PL, Thierry A-M, Glowinski J, Deniau J-M, Gioanni Y (2008) Dopamine modulates temporal dynamics of feedforward inhibition in rat prefrontal cortex in vivo. *Cereb Cortex* 18:2251–2262.
21. Buzsáki G (2010) Neural syntax: Cell assemblies, synapsembles, and readers. *Neuron* 68:362–385.
22. Gray CM, Singer W (1989) Stimulus-specific neuronal oscillations in orientation columns of cat visual cortex. *Proc Natl Acad Sci USA* 86:1698–1702.
23. Heidbreder CA, Groenewegen HJ (2003) The medial prefrontal cortex in the rat: Evidence for a dorso-ventral distinction based upon functional and anatomical characteristics. *Neurosci Biobehav Rev* 27:555–579.
24. Isomura Y, et al. (2006) Integration and segregation of activity in entorhinal-hippocampal subregions by neocortical slow oscillations. *Neuron* 52:871–882.
25. Siapas AG, Wilson MA (1998) Coordinated interactions between hippocampal ripples and cortical spindles during slow-wave sleep. *Neuron* 21:1123–1128.
26. Sirota A, Csicsvari J, Buhl D, Buzsáki G (2003) Communication between neocortex and hippocampus during sleep in rodents. *Proc Natl Acad Sci USA* 100:2065–2069.
27. Wierzynski CM, Lubenov EV, Gu M, Siapas AG (2009) State-dependent spike-timing relationships between hippocampal and prefrontal circuits during sleep. *Neuron* 61: 587–596.
28. Cash SS, et al. (2009) The human K-complex represents an isolated cortical down-state. *Science* 324:1084–1087.
29. Battaglia FP, Sutherland GR, McNaughton BL (2004) Hippocampal sharp wave bursts coincide with neocortical "up-state" transitions. *Learn Mem* 11:697–704.
30. Sirota A, et al. (2008) Entrainment of neocortical neurons and gamma oscillations by the hippocampal theta rhythm. *Neuron* 60:683–697.
31. Sejnowski TJ, Destexhe A (2000) Why do we sleep? *Brain Res* 886:208–223.
32. Contreras D, Destexhe A, Sejnowski TJ, Steriade M (1996) Control of spatiotemporal coherence of a thalamic oscillation by corticothalamic feedback. *Science* 274:771–774.
33. Destexhe A, Contreras D, Steriade M (1999) Cortically-induced coherence of a thalamic-generated oscillation. *Neuroscience* 92:427–443.
34. Hartwich K, Pollak T, Klausberger T (2009) Distinct firing patterns of identified basket and dendrite-targeting interneurons in the prefrontal cortex during hippocampal theta and local spindle oscillations. *J Neurosci* 29:9563–9574.
35. Destexhe A, Hughes SW, Rudolph M, Crunelli V (2007) Are corticothalamic 'up' states fragments of wakefulness? *Trends Neurosci* 30:334–342.
36. Destexhe A, Contreras D, Steriade M (1999) Spatiotemporal analysis of local field potentials and unit discharges in cat cerebral cortex during natural wake and sleep states. *J Neurosci* 19:4595–4608.
37. Harris KD, Csicsvari J, Hirase H, Dragoi G, Buzsáki G (2003) Organization of cell assemblies in the hippocampus. *Nature* 424:552–556.
38. Bartos M, Vida I, Jonas P (2007) Synaptic mechanisms of synchronized gamma oscillations in inhibitory interneuron networks. *Nat Rev Neurosci* 8:45–56.
39. Benchenane K, Tiesinga PH, Battaglia FP (2011) Oscillations in the prefrontal cortex: A gateway to memory and attention. *Curr Opin Neurobiol* 21:475–485.
40. Bragin A, et al. (1995) Gamma (40-100 Hz) oscillation in the hippocampus of the behaving rat. *J Neurosci* 15:47–60.
41. Tort AB, et al. (2008) Dynamic cross-frequency couplings of local field potential oscillations in rat striatum and hippocampus during performance of a T-maze task. *Proc Natl Acad Sci USA* 105:20517–20522.
42. Canolty RT, et al. (2006) High gamma power is phase-locked to theta oscillations in human neocortex. *Science* 313:1626–1628.
43. Sirota A, Buzsáki G (2005) Interaction between neocortical and hippocampal networks via slow oscillations. *Thalamus Relat Syst* 3:245–259.
44. Battaglia FP, Benchenane K, Sirota A, Pennartz CM, Wiener SI (2011) The hippocampus: Hub of brain network communication for memory. *Trends Cogn Sci* 15:310–318.
45. Zanos TP, Mineault PJ, Pack CC (2011) Removal of spurious correlations between spikes and local field potentials. *J Neurophysiol* 105:474–486.
46. Contreras D, Timofeev I, Steriade M (1996) Mechanisms of long-lasting hyperpolarizations underlying slow sleep oscillations in cat corticothalamic networks. *J Physiol* 494:251–264.
47. Shu Y, Hasenstaub A, McCormick DA (2003) Turning on and off recurrent balanced cortical activity. *Nature* 423:288–293.
48. Maviel T, Durkin TP, Menzaghi F, Bontempi B (2004) Sites of neocortical reorganization critical for remote spatial memory. *Science* 305:96–99.
49. Huber R, Ghilardi MF, Massimini M, Tononi G (2004) Local sleep and learning. *Nature* 430:78–81.